IEEE Access
Multidisciplinary | Rapid Review | Open Access Journal

Received February 19, 2021, accepted February 26, 2021, date of publication March 2, 2021, date of current version March 9, 2021.

Digital Object Identifier 10.1109/ACCESS.2021.3063364

Digital Predistortion Utilizing Over-the-Air Feedback for Phased Arrays

YING LIU, (Member, IEEE), XIANGJIE XIA, (Graduate Student Member, IEEE), QIANNAN ZHANG, WENSHENG PAN, (Member, IEEE), SHIHAI SHAO, (Member, IEEE), AND YOUXI TANG

National Key Laboratory of Science and Technology on Communications, University of Electronic Science and Technology of China, Chengdu 611731, China

Corresponding author: Ying Liu (liuying850613@uestc.edu.cn)

This work was supported in part by the National Natural Science Foundation of China under Grant 62071094, Grant U19B2014, Grant 61771107, Grant 61701075, Grant 61601064, and Grant 61531009; and in part by the National Key Research and Development Program of China under Grant 2018YFB1801903.

ABSTRACT In this paper, an efficient digital predistortion (DPD) architecture utilizing over-the-air (OTA) feedback is presented to linearize phased array transmitters. It places one additional observation antenna (OA) in the far field to capture the combined signal of the array outputs and uses the combined signal to build a nonlinear model that describes the joint nonlinear distortions of all the power amplifiers (PAs) in the phased array. Then, a corresponding DPD model is extracted by the typical indirect learning method to linearize the phased array. After introducing this DPD architecture, the relationship between the OA position and the performance of the extracted DPD model is specifically explored, and two significant results are found. First, when the OA is perfectly colocated in the main beam direction, the DPD coefficients extracted with an arbitrary steering angle for the phased array are also applicable to any other steering angle. Second, when the OA is not perfectly placed in the main beam direction, the linearization performance for the extracted DPD coefficients will degrade as the OA placement mismatch increases, and the phased array has an optimum steering angle at which the OA placement mismatch has a minimal influence on the DPD performance. Based on the above two results, a new DPD training strategy is proposed, which extracts only one set of DPD coefficients by making the phased array point at the optimum steering angle. The advantages of the proposed strategy are that the OA can be placed in a relatively wide range of positions and that the extracted coefficients will be applicable to any other steering angle. The two results and the proposed DPD training strategy are verified by simulations, which are conducted on a 1×4 uniform linear array (ULA) and a 4×4 uniform rectangular array (URA).

INDEX TERMS Digital predistortion, phased arrays, antenna radiation patterns, beamforming, single-feedback circuits.

I. INTRODUCTION

Massive multiple-input multiple-output (mMIMO) is one of the most promising techniques in fifth-generation (5G) networks due to its potential in improving the reliability and capacity of wireless communication systems [1]–[4]. Among all mMIMO structures, phased array systems, which adopt radio frequency (RF) beamformers, play an important role since they provide accurate beamforming, flexible beam scanning, and considerable gain [5]–[7]. To achieve high efficiency, power amplifiers (PAs) of multiple RF branches in phased array transmitters usually work in the saturation region where the PA's nonlinearity becomes strong [8], [9]. The nonlinearity of the PA reduces the transmitted signal's quality and causes spectral regrowth [10], [11]. Therefore, to avoid violating communication standard requirements and spectrum regulations, it is imperative to compensate for the nonlinearities of the PAs in phased arrays [12]–[14].

Digital predistortion (DPD) methods have demonstrated excellent performance in linearizing PAs in single-input single-output (SISO) systems. Hence, it is natural to consider adopting the DPD methods in phased array transmitters for the linearization of PAs [15]–[17]. Lee in [15] built a separate feedback loop to estimate each branch's PA model

The associate editor coordinating the review of this manuscript and approving it for publication was Debdeep Sarkar.

and calculate the corresponding DPD coefficients. However, the adoption of multiple feedback loops inevitably increases the complexity of the system's implementation, especially when the number of transmitter antennas increases. Ng in [16] placed an extra observation antenna (OA) in the far field to obtain the combined signal of the phased array, which was regarded as over-the-air (OTA) feedback [18]. Then, all the PA branches in the array can be considered as constituting a joint nonlinear model that is estimated from the combined signal, and the corresponding DPD model can be constructed to linearize the joint nonlinear model. This OTA feedback method performs the DPD training in advance where the user transmission is suspended. After the DPD training is over, the user transmission is turned back on, and the phased array adopts the trained DPD coefficients for linearization, no matter how the user moves. The OTA feedback method is a potential solution for DPD linearization in a phased array given that only one feedback loop is required. However, the issue of OA placement remains unresolved, and OA is usually considered to be perfectly placed in the main beam direction[1] in the literature. As demonstrated in [16], three sets of DPD coefficients are required to cover a steering-angle range of 120 degrees due to the inherent OA placement mismatch in practice.

This paper first presents a DPD architecture with OTA feedback for a phased array and then studies the issue of OA placement. To relax the requirement of OA placement and reduce the complexity of DPD coefficient extraction, the relationship between the OA position and DPD performance is specifically explored. As a result, a new DPD training strategy is developed, where the OA can be placed in a relatively wide range and only one set of DPD coefficients are extracted to cover all the steering angles for the phased array. The contributions of this work are summarized below.

1) *Performance Analysis Without an OA Placement Mismatch:* The DPD performance is analyzed in an ideal scenario without an OA placement mismatch; i.e., the OA is perfectly placed in the main beam direction. It is demonstrated that the combined signal in the main beam direction, which is captured by the OA in an ideal scenario, is independent of the steering angles of the phased array. Therefore, the DPD coefficients extracted from the combined signal (which is captured by the OA) are the same for different steering angles. Under this consideration, we give the result that the DPD coefficients trained at one steering angle will be applicable to any other steering angle in an ideal scenario, and only one set of DPD coefficients needs to be trained to cover all the steering angles.
2) *Performance Analysis with an OA Placement Mismatch:* When there is an OA placement mismatch, i.e., the OA is not perfectly placed in the main beam direction, we show that the DPD performance degrades as the OA placement mismatch increases. In addition, there exists an optimum steering angle where the OA can be placed in the largest range around the main beam direction. The DPD coefficients extracted within this range show satisfactory linearization performance. This result implies that the OA position will be flexible as long as the phased array is pointed at the optimum steering angle.
3) *A New DPD Extraction Strategy:* Based on the above two analyses, a new DPD training strategy is proposed, where only one set of DPD coefficients is extracted and the OA can be placed in a relatively wide range. In the proposed strategy, the phased array is pointed at the optimum steering angle, and the OA is placed in a position within a range around the main beam direction. The signal captured by the OA is used to extract one set of DPD coefficients for the linearization of the phased array. The extracted set of coefficients is applicable to all the other steering angles.
4) *Simulation Verification Using Two Typical Arrays:* The simulation results for a 1×4 uniform linear array (ULA) and a 4×4 uniform rectangular array (URA) are provided to validate the analyses of the OA placement and demonstrate the proposed DPD extraction strategy. It is verified that the proposed DPD extraction strategy is effective in these two common antenna scenarios of a ULA and URA. After DPD linearization with coefficient extraction as in the proposed strategy, the adjacent channel power ratio (ACPR) performance can be improved to less than -55 dBc, and the error vector magnitude (EVM) performance can be improved to less than 3.5%.

The remainder of the paper is organized as follows: The system architecture for phased array DPD is presented in Section II. Section III explores the relationship between OA placement and DPD performance and proposes a new DPD extraction strategy that has low complexity. The simulation results and the corresponding analyses are given in Section IV, and Section V concludes this paper.

II. DIGITAL PREDISTORTION ARCHITECTURE

The system architecture is shown in Fig. 1, where the main beam of the phased array points to a steering angle. An additional OA is placed at the corresponding angle in the far field to obtain the main beam signal. Here, the OA is considered to be perfectly placed in the main beam direction to simplify the system architecture description. By using the observed signal and the input signal of the phased array, a joint nonlinear model is first built for the phased array, and then the corresponding DPD model coefficients are extracted.

A. NONLINEAR MODEL FOR THE PHASED ARRAY

As shown in Fig. 1, after DPD, DAC, and mixing, the baseband source signal u(n) yields the RF signal x(t). Then, $x(t)$ is fed to the phased array with L branches, where α_l and φ_l are the amplitude attenuator and the phase shifter for the

[1] Here, the main beam direction is the direction of the intended receiver, and it is also the direction pointed by the steering angle of the phased array.

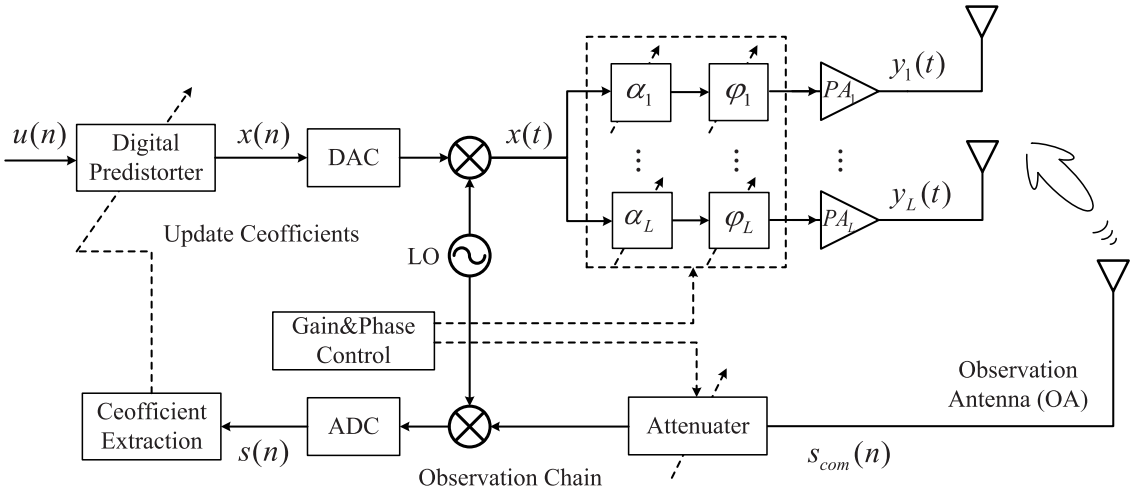

FIGURE 1. DPD architecture with OTA feedback for phased arrays.

l-th branch, respectively. To characterize the nonlinear PA distortion of the l-th branch, the widely used memory polynomial (MP) model [19] is adopted here. Therefore, the output of the l-th PA is given by

$$y_l(n) = \sum_{k=0}^{K_l-1} \sum_{q=0}^{Q_l-1} \alpha_l^{k+1} e^{j\varphi_l} w_{lkq} x(n-q)|x(n-q)|^k, \quad (1)$$

where α_l^{k+1} is the $k+1$-th power of α_l, w_{lkq} are the PA model coefficients with the k-th nonlinear order and q-th memory depth for the l-th branch, and K_l and Q_l are the maximum nonlinear order and the memory depth, respectively.

In this paper, we consider two typical antenna scenarios (i.e., a ULA and URA), where the ULA can be regarded as a simplified version of the URA. Therefore, in the following, we will present only the beamforming principles and the DPD method for the URA, which are also applicable to the ULA. The layout and the antenna pattern for the URA are shown in Fig. 2. After propagating through the air, the l-th branch output $y_l(n)$ becomes $s_l(n)$ with a spatial angle (θ, φ):

$$\begin{aligned} s_l(n) &= y_l(n) e^{j(a\beta d_1 \sin\varphi \cos\theta + b\beta d_2 \sin\theta)} \\ &= y_l(n) e^{j\phi_l}, \end{aligned} \quad (2)$$

where $\beta = 2\pi/\lambda$ is the propagation constant; a and b are the indices of the antenna unit along the y-axis and the z-axis, respectively; and d_1 and d_2 are the spatial distances between the adjacent elements of the array along the y-axis and the z-axis, respectively. For the l-th antenna element, we can use $(a \times d_1, b \times d_2)$ to represent its coordinates, as shown in Fig. 2. When the main beam direction points to (θ_M, φ_M), the propagation phase difference ϕ_l becomes

$$\phi_l = a\beta d_1 \sin\varphi_M \cos\theta_M + b\beta d_2 \sin\theta_M, \quad (3)$$

and we therefore have

$$\varphi_l = -(a\beta d_1 \sin\varphi_M \cos\theta_M + b\beta d_2 \sin\theta_M) = -\phi_l. \quad (4)$$

Then, the combined signal $s_{com}(n)$ in the main beam direction (θ_M, φ_M) is given as

$$\begin{aligned} s_{com}(n) &= \sum_{l=0}^{L-1} s_l(n) \\ &= \sum_{l=0}^{L-1} y_l(n) e^{j\phi_l} \\ &= \sum_{k=0}^{K_l-1} \sum_{q=0}^{Q_l-1} \sum_{l=0}^{L-1} e^{j(\varphi_l+\phi_l)} \alpha_l^{k+1} w_{lkq} x(n-q)|x(n-q)|^k \\ &= \sum_{k=0}^{K_l-1} \sum_{q=0}^{Q_l-1} \sum_{l=0}^{L-1} \alpha_l^{k+1} w_{lkq} x(n-q)|x(n-q)|^k. \end{aligned} \quad (5)$$

After normalization of the combined signal $s_{com}(n)$, we have

$$\begin{aligned} s(n) &= \frac{1}{G} s_{com}(n) \\ &= \frac{1}{G} \sum_{k=0}^{K_l-1} \sum_{q=0}^{Q_l-1} \sum_{l=0}^{L-1} \alpha_l^{k+1} w_{lkq} x(n-q)|x(n-q)|^k \\ &= \sum_{k=0}^{K_l-1} \sum_{q=0}^{Q_l-1} \frac{1}{G} \sum_{l=0}^{L-1} \alpha_l^{k+1} w_{lkq} x(n-q)|x(n-q)|^k \\ &= \sum_{k=0}^{K-1} \sum_{q=0}^{Q-1} w_{kq} x(n-q)|x(n-q)|^k, \end{aligned} \quad (6)$$

where $s(n)$ is the normalized combined signal. K and Q denote the maximum nonlinear order and memory depth for the overall single non-linear model. K is the maximum value in $K_1, K_2, \ldots, K_L$, and Q is the maximum value in $Q_1, Q_2, \ldots, Q_L$. G is the desired gain factor of the phased array, and it is used to normalize the measured combined signal data. $w_{kq} = 1/G\Sigma_{l=0}^{L-1} \alpha_l^{k+1} w_{lkq}$, and w_{kq} is the coefficient with the k-th nonlinear order and q-th memory depth for the single nonlinear model.

From (6), it can be found that a joint nonlinear model with the coefficients w_{kq} can be used to model the combined

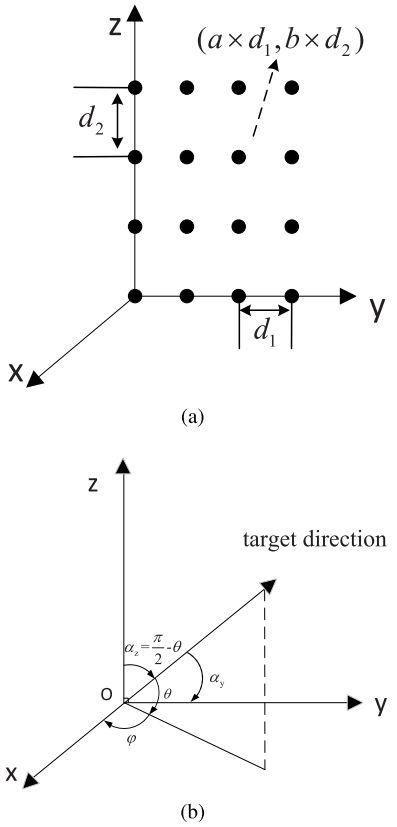

FIGURE 2. Illustration of a uniform rectangular array (URA). (a) The array orientation, with 16 antenna elements uniformly located in the *yoz*-plane in a rectangular shape; (b) the target direction of the array pattern in the same coordinates.

signal $s(n)$. This joint nonlinear model actually represents the overall nonlinearity for a phased array with L branch nonlinearities. Note that model (6) is linear in its coefficients, and hence, w_{kq} can be estimated by the least squares (LS) method introduced below.

We simply consider that $s(n)$ is captured by the OA that is perfectly placed in the main beam direction. The collection of captured samples for $s(n)$ is written as a vector $\mathbf{s}$, and the corresponding collection of the samples for the input signal $x(n)$ is written as a vector $\mathbf{x}$. Then, the nonlinear model (6) can be rewritten in matrix form as

$$\mathbf{s} = \mathbf{X}\mathbf{w}, \tag{7}$$

where $\mathbf{X}$ is the data matrix constructed from the samples in $\mathbf{x}$ and the basis function of model (6), and $\mathbf{w}$ is the vector representing the collection of the coefficients w_{kq} of model (6). The LS solution to (7) is given as

$$\hat{\mathbf{w}} = (\mathbf{X}^H\mathbf{X})^{-1}\mathbf{X}^H\mathbf{s}, \tag{8}$$

where $\hat{\mathbf{w}}$ is the estimated coefficient and $(\cdot)^H$ denotes the complex conjugate transpose. By using $\hat{\mathbf{w}}$, the combined output signal of the phased array can be reconstructed as

$$\hat{s}(n) = \sum_{k=0}^{K_l-1}\sum_{q=0}^{Q_l-1} \hat{w}_{kq}x(n-q)|x(n-q)|^k, \tag{9}$$

where $\hat{w}_{kq}$ is the coefficient element in $\hat{\mathbf{w}}$.

B. DPD COEFFICIENT EXTRACTION AND PA LINEARIZATION

After the overall nonlinear model for the phased array is built by (9), the corresponding DPD model can be extracted by using the typical indirect learning method [20]–[22]. We swap the input $x(n)$ and the output $\hat{s}(n)$ of the PA model (9) to obtain the DPD model function as

$$x(n) = \sum_{k=0}^{K_l-1}\sum_{q=0}^{Q_l-1} \omega_{kq}\hat{s}(n-q)|\hat{s}(n-q)|^k, \tag{10}$$

where ω_{kq} is the set of DPD model coefficients. Similar to (7), the DPD model (10) can be rewritten in matrix form as

$$\mathbf{x} = \hat{\mathbf{S}}\boldsymbol{\omega}, \tag{11}$$

where $\hat{\mathbf{S}}$ is the data matrix corresponding to the signal samples of $\hat{s}(n)$, which is similar to $\mathbf{X}$, and $\boldsymbol{\omega}$ is the vector representing the collection of the coefficients ω_{kq} of model (10). The LS solution to (11) is given as

$$\hat{\boldsymbol{\omega}} = (\hat{\mathbf{S}}^H\hat{\mathbf{S}})^{-1}\hat{\mathbf{S}}^H\mathbf{x}, \tag{12}$$

where $\hat{\boldsymbol{\omega}}$ is the estimated DPD coefficient.

The extracted DPD coefficients $\hat{\boldsymbol{\omega}}$ can be used to linearize the PA array. The source signal $x(n)$ is first fed to the DPD model to obtain the predistorted signal as

$$x_{\mathrm{DPD}}(n) = \sum_{k=0}^{K_l-1}\sum_{q=0}^{Q_l-1} \hat{\omega}_{kq}x(n-q)|x(n-q)|^k. \tag{13}$$

Then, the predistorted signal $x_{\mathrm{DPD}}(n)$ is fed to the phased array for linearization. Note that the above model extraction and results rely on the hypothesis that the OA is perfectly placed in the main beam direction and $s(n)$ is properly captured by the OA. In practice, an OA placement mismatch always exists. In the literature, the OA position and the main beam direction are as close as possible, which is inconvenient and time-consuming. In addition, a number of DPD coefficient sets are required for different steering angles, as reported in [16].

III. OA PLACEMENT EXPLORATION

This section explores the issue of OA placement. In particular, the relationship between the OA position and the performance of the extracted DPD model is analyzed. We first analyze the DPD performance in an ideal scenario without an OA placement mismatch and then study the DPD performance with an OA placement mismatch. Finally, a low-complexity strategy is proposed to extract the DPD model.

A. PERFORMANCE ANALYSIS WITHOUT AN OA PLACEMENT MISMATCH

In an ideal scenario where the OA is perfectly placed in the main beam direction, the OA will capture the combined signal in the main beam direction. As demonstrated by (3), (4), and (5), the propagation phase difference ϕ_l at the steering angle (θ_M, φ_M) is compensated by the phase shifter φ_l in the

phased array. Therefore, the combined signal (normalized) in the main beam direction is again given as

$$s(n) = \sum_{k=0}^{K_l-1}\sum_{q=0}^{Q_l-1}\frac{1}{G}\sum_{l=0}^{L-1}\alpha_l^{k+1}w_{lkq}x(n-q)|x(n-q)|^k. \quad (14)$$

According to (14), $s(n)$ is independent of the steering angle (θ_M, φ_M). Therefore, the DPD model coefficients, which are extracted from $s(n)$, will be the same for different steering angles.

Remark 1: As long as the OA is perfectly placed in the main beam direction, the DPD coefficients trained at one steering angle will be applicable to any other steering angle, and only one set of DPD coefficients needs to be trained to cover all the steering angles.

B. PERFORMANCE ANALYSIS WITH AN OA PLACEMENT MISMATCH

Remark 1 shows that only one set of DPD coefficients needs to be trained in an ideal scenario. However, it is difficult to perfectly place the OA in the main beam direction in practice due to influences such as imperfect measurements, environmental limitations, and inaccurate phase shifters. Hence, OA placement mismatch is almost unavoidable in practice.

When the OA is placed at a specific angle denoted by (θ, φ), which deviates from the steering angle (θ_M, φ_M), the propagation phase difference is $\phi_l = a\beta d_1 \sin\varphi\cos\theta + b\beta d_2 \sin\theta$, and the phase shift is $\varphi_l = -(a\beta d_1 \sin\varphi_M \cos\theta_M + b\beta d_2 \sin\theta_M) \neq -\phi_l$. Then, the combined signal observed by the OA is given as

$$\begin{aligned} s_{com}^{\theta}(n) &= \sum_{l=0}^{L-1} s_l(n) \\ &= \sum_{l=0}^{L-1} y_l(n)e^{j\phi_l} \\ &= \sum_{l=0}^{L-1}\sum_{k=0}^{K_l-1}\sum_{q=0}^{Q_l-1} e^{j(\phi_l+\varphi_l)}\alpha_l^{k+1}w_{lkq}x(n-q)|x(n-q)|^k. \end{aligned} \quad (15)$$

Additionally, considering the normalization of $s_{com}^{\theta}(n)$, we have

$$\begin{aligned} s_\theta(n) &= \frac{1}{g}s_{com}^{\theta}(n) \\ &= \frac{1}{g}\sum_{k=0}^{K_l-1}\sum_{q=0}^{Q_l-1}\sum_{l=0}^{L-1} e^{j(\phi_l+\varphi_l)}\alpha_l^{k+1}w_{lkq}x(n-q)|x(n-q)|^k \\ &= \sum_{k=0}^{K_l-1}\sum_{q=0}^{Q_l-1}\lambda_{kq}x(n-q)|x(n-q)|^k, \end{aligned} \quad (16)$$

where g is the gain normalization factor of the phased array at the angle (θ, φ) and $\lambda_{kq} = 1/g\Sigma_{l=0}^{l-1}e^{j(\phi_l+\varphi_l)}\alpha_l^{k+1}w_{lkq}$ is the coefficient of the joint nonlinear model for the PA array.

Since the steering angle is (θ_M, φ_M) and the OA is placed at the angle (θ, φ), there are mismatches between the main beam signal $s(n)$ and the combined signal $s_\theta(n)$ observed by the OA. Therefore, if we use $s_\theta(n)$ to train the DPD coefficients and use the trained DPD coefficients to linearize $s(n)$, the DPD performance will degrade due to the presence of the OA placement mismatch. According to (6) and (16), the error signal between $s(n)$ and $s_\theta(n)$ is defined as

$$\begin{aligned} e^{\theta}(n) &= s(n) - s_\theta(n) \\ &= \sum_{k=0}^{K_l-1}\sum_{q=0}^{Q_l-1}(w_{kq} - \lambda_{kq})x(n-q)|x(n-q)|^k \\ &= \sum_{k=0}^{K_l-1}\sum_{q=0}^{Q_l-1}\sum_{l=0}^{L-1}\alpha_l^{k+1}\left(\frac{1}{G} - \frac{1}{g}e^{j(\phi_l+\varphi_l)}\right) \\ &\quad \times w_{lkq}x(n-q)|x(n-q)|^k, \end{aligned} \quad (17)$$

where $\varphi_l = -(a\beta d_1 \sin(\varphi_M)\cos(\theta_M) + b\beta d_2 \sin(\theta_M))$ and $\phi_l = a\beta d_1 \sin(\varphi)\cos(\theta) + b\beta d_2 \sin(\theta)$. Through simulations, we find that as long as the amplitude of the error $e^{\theta}(n)$ is small, the DPD coefficients trained by $s_\theta(n)$ will still be effective for the linearization of the phased array (note that the linearization of the phased array specifically represents the linearization of the main-beam-direction signal $s(n)$).

The error $e^{\theta}(n)$ is related to the steering angle (θ_M, φ_M) and the OA placement angle (θ, φ). We present array patterns with steering angles of $(\theta_M = 0°, \varphi_M = 0°)$ and $(\theta_M = 60°, \varphi_M = 60°)$ to simply illustrate $e^{\theta}(n)$. Fig. 3 shows an array pattern with a steering angle of $(\theta_M = 0°, \varphi_M = 0°)$. Fig. 3 indicates that if the OA is perfectly placed in the main beam direction, i.e., $(\theta = 0°, \varphi = 0°)$, the combined signal captured by the OA, i.e., $s(n)$, has the maximum amplitude. If the OA is placed in the other direction, i.e., $(\theta \neq 0°, \varphi \neq 0°)$, the amplitude of $s_\theta(n)$, which is the combined signal captured by the OA, will gradually decrease. We have

$$\begin{aligned} \left|e^{\theta}(n)\right| &= |s(n) - s_\theta(n)| \\ &\geqslant ||s(n)| - |s_\theta(n)|| = |s(n)| - |s_\theta(n)|. \end{aligned} \quad (18)$$

Equation (18) indicates that on the whole, if the amplitude of $s_\theta(n)$ decreases, the amplitude of $e^{\theta}(n)$ will increases. Therefore, the amplitude of $e^{\theta}(n)$ will increase if (θ, φ) deviates from $(0, 0)$. Fig. 3 also shows the power of $e^{\theta}(n)$ (i.e., $\left|e^{\theta}(n)\right|^2$), which also demonstrates the increase of $\left|e^{\theta}(n)\right|$ when (θ, φ) deviates from $(0, 0)$. Note that the array pattern uses the dB unite while the power of $e^{\theta}(n)$ does not adopts the dB unit because the existence of 0 for $\left|e^{\theta}(n)\right|$. Fig. 4 presents an array pattern and the power of $e^{\theta}(n)$ with a steering angle of $(\theta_M = 60°, \varphi_M = 60°)$. Due to the different steering angles, Fig. 4 and Fig. 3 show different array patterns. Similarly, the signal captured by the OA will have the maximum amplitude if the OA is perfectly placed in the main beam direction, i.e., $(\theta = 60°, \varphi = 60°)$.

Fig. 3 and Fig. 4 both indicate that the amplitude of $e^{\theta}(n)$ increases when the OA placement angle (θ, φ) deviates from the steering angle (θ_M, φ_M). In addition, compared with Fig. 3 showing $(\theta_M = 0°, \varphi_M = 0°)$, Fig. 4 showing

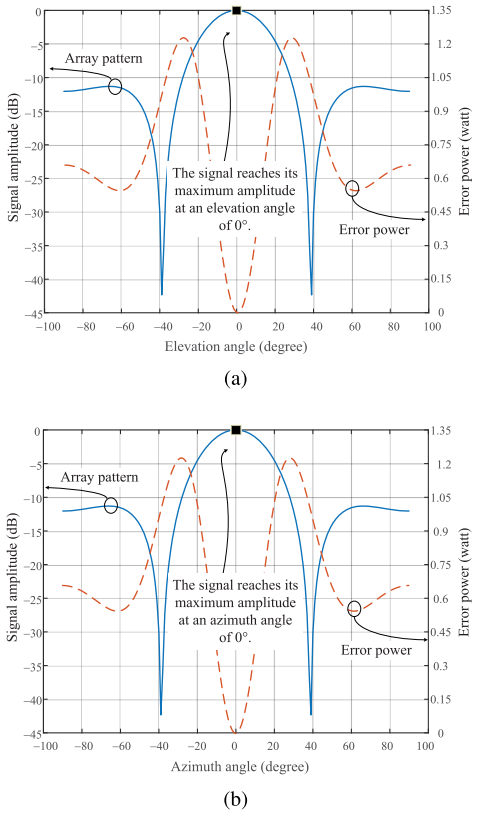

FIGURE 3. Antenna array pattern and error $e^{\theta}(n)$ power at the steering angle ($\theta = 0°$, $\varphi = 0°$). (a) Phased array pattern in which the azimuth angle is fixed at 0°; (b) phased array pattern in which the elevation angle is fixed at 0°.

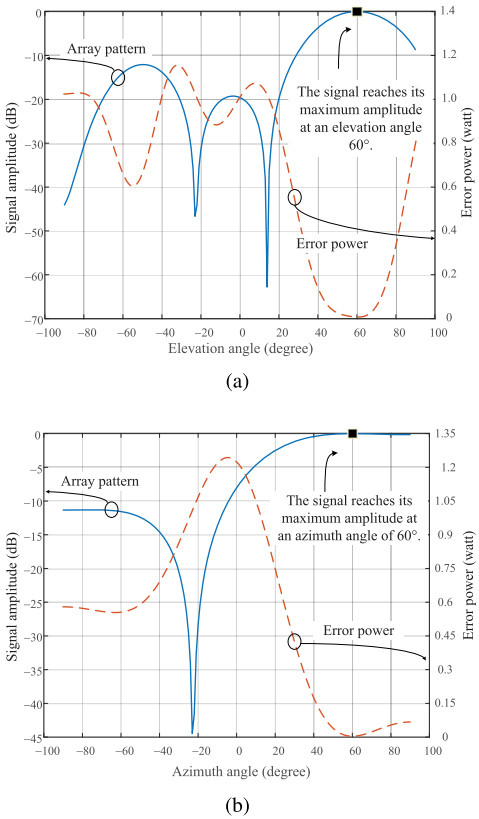

FIGURE 4. Antenna array pattern and error $e^{\theta}(n)$ power at the steering angle ($\theta = 60°$, $\varphi = 60°$). (a) Phased array pattern in which the azimuth angle is fixed at 60°; (b) phased array pattern in which the elevation angle is fixed at 60°.

($\theta_M = 60°$, $\varphi_M = 60°$) has the property that the signal amplitude of the array pattern changes more slowly around (θ_M, φ_M), and hence, the amplitude of $e^{\theta}(n)$ also improves more slowly. This implies that for different steering angles, the amplitude of $e^{\theta}(n)$ increases at different speeds around (θ_M, φ_M). Therefore, it is natural to consider that there exists an optimum steering angle, written as (θ_M^*, θ_M^*), where the amplitude of $e^{\theta}(n)$ increases slowest around (θ_M^*, θ_M^*). It is difficult to directly derive (θ_M^*, θ_M^*), and hence, we search for the optimum such steering angle (θ_M^*, θ_M^*) by drawing array patterns at different steering angles. We find that the optimum steering angle is (60°, 60°). In fact, the beamwidth is different for different steering angles. On the whole, the steering angle of (60°, 60°) has almost the widest beamwidth. Hence, the OA can be placed in a widest range to measure the combined signal of the array outputs when the steering angle is pointed at (60°, 60°).

The DPD coefficients can be trained by making the phased array point to this optimum steering angle (60°, 60°). In such a case, if the OA is placed around the main beam direction of (60°, 60°), the combined signal captured by the OA will have a similar amplitude given that the array patterns change slowly around (60°, 60°). Through simulations, we find that the OA can be placed in a range of ($60° \pm 10°$, $60° \pm 10°$), where the linearization results satisfy the communication standards given by the 3rd generation partnership project (3GPP) [23], [24]. The details of these simulations are reported in Section IV (simulation section).

Remark 2: The linearization performance of the extracted DPD model degrades as the OA placement mismatch increases. Furthermore, there exists an optimum steering angle for the phased array, where the OA can be placed in the largest range around the main beam direction under the condition that the DPD performance remains at an acceptable level. Specifically, this optimum steering angle is (60°, 60°).

C. PROPOSED DPD TRAINING STRATEGY

Based on the above two results, a DPD training strategy is proposed for the phased array. First, according to *Remark 1* of Subsection III. A, the DPD model extracted at one steering angle is also applicable to other steering angles. Second, according to *Remark 2* of Subsection III. B, when the steering angle of the phased array is pointed at (60°, 60°), the OA can be placed in a large range around (60°, 60°), where the DPD performance remains acceptable. Therefore, we summarize the proposed DPD training strategy as follows:

- The user transmission is suspended.
- The steering angle of the phased array is pointed at (60°, 60°).

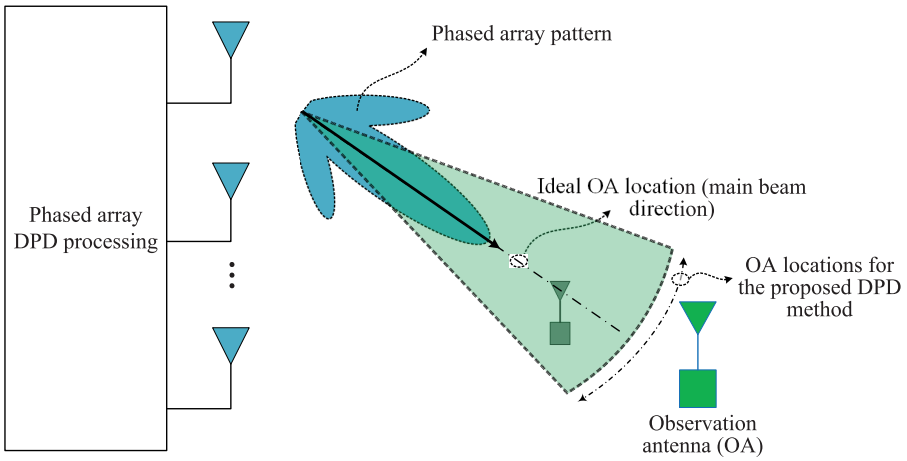

FIGURE 5. OA placement requirements for different DPD methods, where the OA is placed in a narrow range around the main beam direction for conventional methods. In contrast, the OA can be placed in a wide range around the main beam direction for the proposed DPD training strategy.

- The OA is placed in a range around the main beam direction of (60°, 60°). This range can be set according to the communication standard suggested by 3GPP.
- The combined signal is captured by the OA and is applied to train one set of DPD model coefficients to linearize the phased array at all other steering angles.
- The user transmission is turned back on. The user position can change arbitrarily, and the steering angle of the phased array changes accordingly. The phased array always uses the extracted DPD coefficients, regardless of the steering angle.

The proposed strategy is superior to the conventional DPD training strategy for the phased array, given that only one set of coefficients needs to be extracted. In addition, the OA can be placed in a relatively wide range of angles, as shown in Fig. 5. In conventional methods, however, the OA is placed in a narrow range around the main beam direction because the steering angle is not pointed at (60°, 60°). Note that influences such as environmental limitations and inaccurate phase shifters can all be regarded as part of the OA placement mismatch. Therefore, the proposed method is able to achieve a robust linearization performance in complicated scenarios.

IV. SIMULATIONS

This section presents the simulation results that verify the analysis in Section III.

A. SIMULATION CONDITIONS

A 256-QAM modulated source signal with a bandwidth of 20 MHz is adopted. The modulated signal is a pulse shaped by a raised cosine filter with a roll-off factor of 0.22. The sampling clock of the pulse-shaping filter is 8 times the symbol rate, and the amplitude attenuator is set as $\alpha_l = 1$. The ACPR is measured with 22 MHz offset and 20 MHz measurement bandwidth. Both the PA model and DPD model use the MP model ($Q_l = 2$, $K_l = 5$). To simulate the different characteristics of PAs, the PA model coefficients for each branch are extracted differently, from measurements of different PAs. The phased arrays adopt uniform omnidirectional antenna elements and apply two widely used antenna layouts, i.e., a 1×4 ULA with equal spacings $d = 0.5\lambda$ and a 4×4 URA with equal spacings $d_1 = d_2 = 0.5\lambda$ [25]–[27].

B. SIMULATIONS FOR THE ULA SCENARIO

1) SIMULATION PROCEDURES

The simulations for the ULA include scenarios with and without an OA placement mismatch. For the scenario without the OA placement mismatch, the steering angle of the phased array is first set to θ_M, and then the OA is placed in the corresponding main beam direction to capture the combined signal. The combined signal is applied to train the DPD model coefficients, which will be used to linearize the phased array with different steering angles.

For the scenario with the OA placement mismatch, the steering angle of the phased array is first set to θ_M, and then the OA is placed at an angle θ that is different from θ_M. The combined signal captured by the OA is applied to train the DPD model coefficients for the linearization of the phased array with a steering angle of θ_M.

2) SIMULATION RESULTS AND ANALYSIS

Fig. 6 shows the result of the scenario without the OA placement mismatch. As depicted, when the OA is perfectly placed in the main beam direction, the DPD coefficients trained at one steering angle will be applicable to any other steering angle. For instance, the DPD model extracted at a steering angle of 0° (or 20°, 40°, 60°) can similarly linearize all the steering angles of 0°, 10°, 20°, 30°, 40°, 50°, and 60°. Fig. 6 verifies *Remark 1* of Subsection III.A.

Fig. 7 shows the results of the scenario with the OA placement mismatch. It can be observed that the DPD performance degrades when the OA deviates from the steering angle. For steering angles of 0°, 20°, 40°, 60°, and 80°, the ACPR performance can change slightly if the OA placement mismatch is within 15°. In particular, the ACPR curve is almost

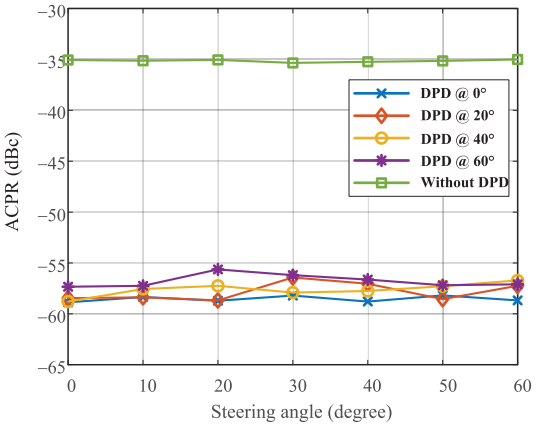

FIGURE 6. ACPR performance versus steering angle, where the OA is perfectly placed in the main beam direction. As depicted, the DPD model extracted at a steering angle of 0° (or 20°, 40°, 60°) can similarly linearize a phased array with steering angles of 0°, 10°, 20°, 30°, 40°, 50°, and 60°.

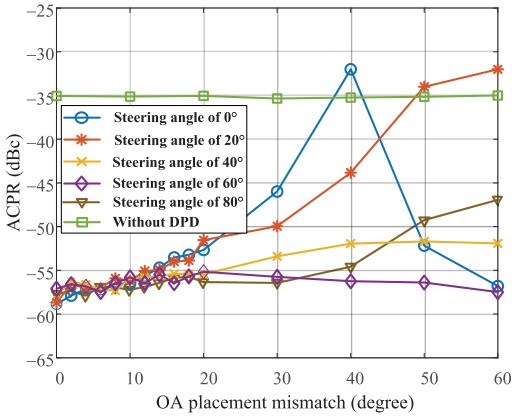

FIGURE 7. ACPR performance versus OA placement mismatch, where the results for steering angles of 0°, 20°, 40°, 60°, and 80° are presented. For a steering angle of 60°, the ACPR changes only slightly as the OA placement mismatch increases.

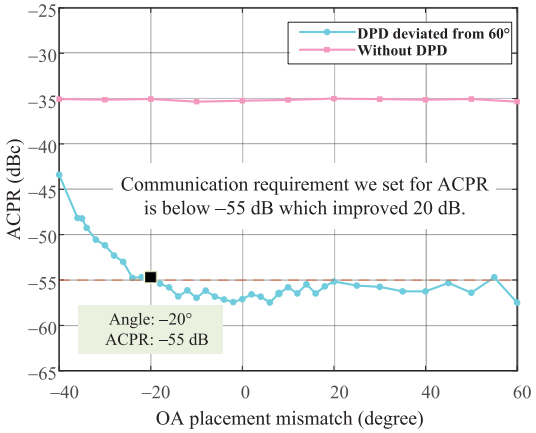

FIGURE 8. ACPR performance versus OA placement mismatch, where the steering angle is fixed at 60°. Here, the OA placement mismatch changes from −20° to 60°.

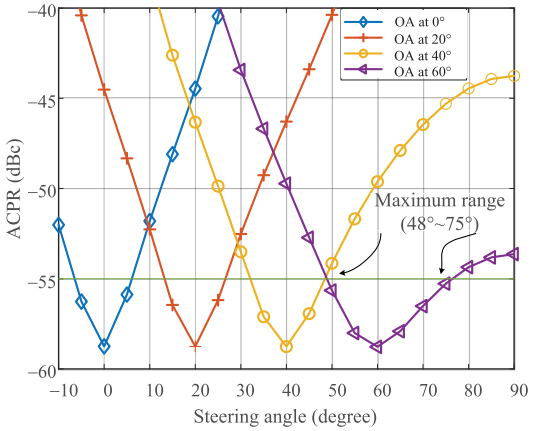

FIGURE 9. DPD performance versus OA placement mismatch under the condition that the OA location is fixed at 0°, 20°, 40°, and 60°.

flat for a steering angle of 60°. Fig. 7 verifies *Remark 2* of Subsection III.B.

Fig. 8 is used to determine the angle range for OA placement in the case of a 60° steering angle. According to the communication standard requirements suggested by 3GPP, the ACPR of the transmitter should be lower than −45 dBc in most cases [23], [24]. Here, the ACPR requirement of −55 dBc is chosen to accommodate the DPD constraints in practice, e.g., the limited computing resources of a field-programmable gate array (FPGA). Fig. 8 shows that the OA can be placed at a wide range of angles, from 40° to 140°, given that in this range, the ACPR performance reaches the desired level of −55 dBc.

Fig. 9 is a supplementary simulation result, which is used to extend the analysis in Section III. In some practical applications, the OA is fixed at a specific angle. The steering angle can be precisely pointed at the OA placement angle to train the DPD coefficients; however, this will also be time consuming. In addition, it is inconvenient to track the status of the PAs if the steering angle is required to be pointed at a specific angle. Hence, we consider training the DPD coefficients with the steering angle scanning an angle range. Fig. 9 shows that if the OA is placed at an angle of 60°, the effective scanning range of the steering angle is maximal (from 48° to 75°). In this maximum scanning range, the ACPR performance reaches −55 dBc. By placing the OA at an angle of 60°, the DPD coefficients can be trained during the process of scanning the phased array. When the steering angle falls within the scanning range of 48° ∼ 75° (i.e., the user receiver is placed within this range), we can fixed the OA at the angle of 60° and train the DPD coefficients in an online process.

In summary, the above simulation results demonstrate the effectiveness of the 60° steering angle for the ULA. When the steering angle is pointed at 60°, the OA can be placed at an angle range from 40° to 140°. When the OA placement mismatch is 85°, the ACPR performance degrades to −48.9 dBc, which violates the requirement of −55 dBc. The DPD model extracted at a steering angle of 60° can also be applied to linearize the phased array with other steering angles, and hence, only one set of DPD coefficients needs to be extracted at the 60° steering angle. It might be thought

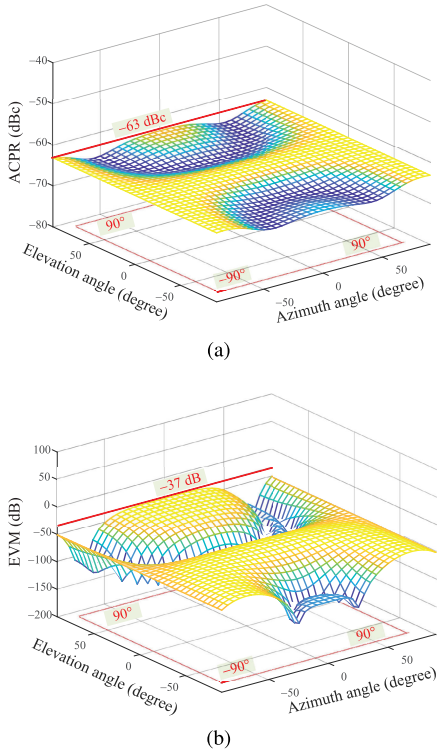

FIGURE 10. DPD performance versus steering angle, where the DPD model is extracted at a steering angle of (60°, 60°). (a) ACPR performance; (b) EVM performance.

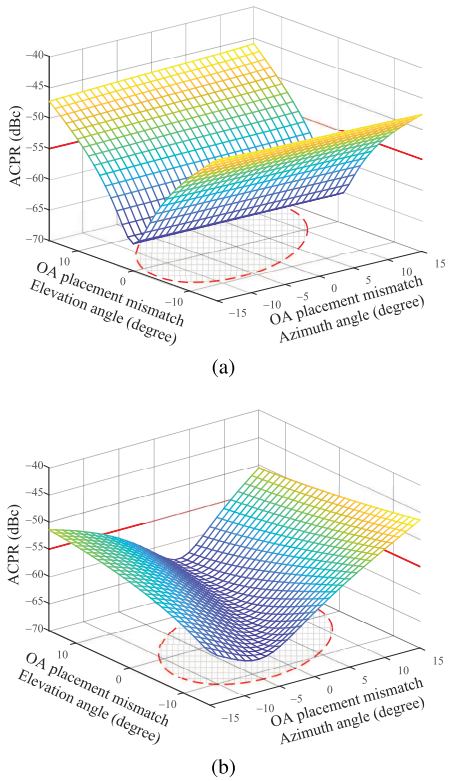

FIGURE 11. ACPR performance versus OA placement mismatch. (a) Results for a steering angle of (0°, 0°); (b) results for a steering angle of (60°, 60°).

that verification of the proposed DPD training strategy is still lacking. In fact, the proposed DPD training strategy is verified through the validations of *Remark 1* and *Remark 2*. The verification results for the proposed DPD training strategy are similar and hence are not presented here.

C. SIMULATIONS FOR THE URA SCENARIO

1) SIMULATION PROCEDURES

The simulations for the URA also include scenarios with and without an OA placement mismatch. For the scenario without the OA placement mismatch, the steering angle of the URA is first set to $(60°, 60°)$, and then the OA is placed in the corresponding main beam direction to capture the combined signal. The combined signal is applied to extract the DPD model, which is used to linearize the URA with steering angles of $(-90°, -90°), (-90°, -80°), \ldots, (-90°, 90°), \ldots, (-80°, -90°), (-80°, -80°), \ldots, (90°, 90°)$.

For the scenario with the OA placement mismatch, the steering angle of the URA is first set to (θ_M, φ_M), and then the OA is placed at an angle (θ, φ) that is different from (θ_M, φ_M). The combined signal captured by the OA is applied to train the DPD model coefficients for the linearization of the phased array with a steering angle of (θ_M, φ_M).

2) SIMULATION RESULTS AND ANALYSIS

Fig. 10 shows the results for the scenario without the OA placement mismatch, where Fig. 10(a) is the ACPR performance and Fig. 10(b) is the EVM performance. As depicted, when the OA is perfectly placed in the main beam direction, the DPD model, which is extracted at a steering angle of $(60°, 60°)$, can be used to effectively linearize the phased array with steering angles covering 360° of space. In particular, the ACPR performances are always improved to below -63 dBc, and the EVM performances are always improved to below 1.5%.

Figs. 11 and 12 show the results for the scenario with the OA placement mismatch. Fig. 11(a) and (b) show the ACPR performance versus OA placement mismatch with steering angles of $(0°, 0°)$ and $(60°, 60°)$, respectively. Fig. 12(a) and (b) show the EVM performance versus OA placement mismatch with steering angles of $(0°, 0°)$ and $(60°, 60°)$, respectively. For a steering angle of $(60°, 60°)$, the OA can be placed in a range of $(60° \pm 10°, 60° \pm 10°)$, where the ACPR and EVM performances remain below -55 dBc and 3.5% (-30 dB), respectively.

In summary, the above simulation results demonstrate the effectiveness of the $(60°, 60°)$ steering angle for the URA. When the steering angle is $(60°, 60°)$, the OA can be placed in a range of $(60° \pm 10°, 60° \pm 10°)$. The DPD model extracted at the steering angle $(60°, 60°)$ can also be applied to linearize the phased array with other steering angles, indicating that only one set of DPD coefficients needs to be extracted at the $(60°, 60°)$ steering angle.

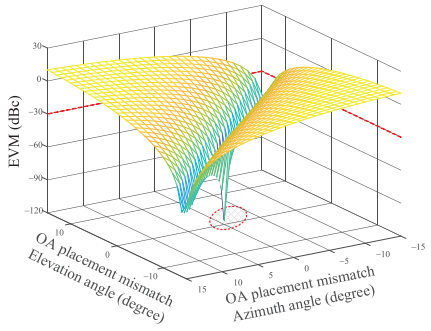

(a)

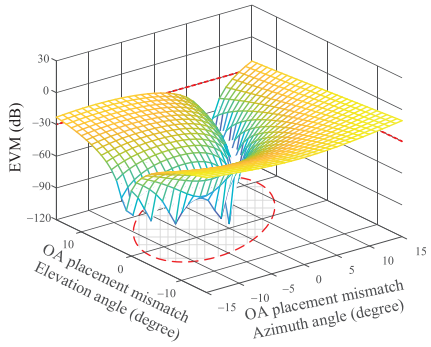

(b)

FIGURE 12. EVM performance versus OA placement mismatch. (a) Results for a steering angle of (0°, 0°); (b) results for a steering angle of (60°, 60°).

V. CONCLUSION

In this paper, an efficient digital predistortion (DPD) architecture utilizing OTA feedback was first introduced, and then the issue of OA placement was explored in detail. The DPD performance was analyzed in two scenarios, with and without the OA placement mismatch, and two significant results were given. The first result is that only one set of DPD coefficients needs to be extracted to cover all steering angles for the phased array. The second result is that the phased array has an optimum steering angle at which the OA can be placed in a wide range. These two results inspired us to propose a new DPD training strategy for the linearization of the phased array. The proposed strategy has the advantages that the OA placement is flexible and that the DPD coefficients can be trained online during the scanning process. The simulation results verified the two results obtained and the proposed DPD training strategy. The DPD method proposed in this paper is more adaptive than previous methods to complicated scenarios such as unstable supply voltages and changing temperatures.

REFERENCES

[1] E. Zeydan, O. Dedeoglu, and Y. Turk, "Experimental evaluations of TDD-based massive MIMO deployment for mobile network operators," *IEEE Access*, vol. 8, pp. 33202–33214, Feb. 2020.

[2] A. Morsali, A. Haghighat, and B. Champagne, "Generalized framework for hybrid analog/digital signal processing in massive and ultra-massive-MIMO systems," *IEEE Access*, vol. 8, pp. 100262–100279, May 2020.

[3] L. Liu, W. Chen, L. Ma, and H. Sun, "Single-PA-feedback digital predistortion for beamforming MIMO transmitter," in *Proc. IEEE Int. Conf. Microw. Millim. Wave Technol. (ICMMT)*, vol. 2, Jun. 2016, pp. 573–575.

[4] S. Noh, J. Song, and Y. Sung, "Fast beam search and refinement for millimeter-wave massive MIMO based on two-level phased arrays," *IEEE Trans. Wireless Commun.*, vol. 19, no. 10, pp. 6737–6751, Oct. 2020.

[5] Q. Lu and C. Yu, "In-band digital predistortion for concurrent dual-broadband phased array transmitters," *IEEE Microw. Wireless Compon. Lett.*, vol. 29, no. 4, pp. 294–296, Apr. 2019.

[6] G. Hu, C. Yu, and X.-W. Zhu, "Digital predistortion model comparison for phased array transmitters with multi-channel time delay," in *Proc. Int. Conf. Microw. Millim. Wave Technol. (ICMMT)*, May 2018, pp. 1–3.

[7] Y. Zhang, Y. Huo, D. Wang, X. Dong, and X. You, "Channel estimation and hybrid precoding for distributed phased arrays based MIMO wireless communications," *IEEE Trans. Veh. Technol.*, vol. 69, no. 11, pp. 12921–12937, Nov. 2020.

[8] X. Liu, Q. Zhang, W. Chen, H. Feng, L. Chen, F. M. Ghannouchi, and Z. Feng, "Beam-oriented digital predistortion for 5G massive MIMO hybrid beamforming transmitters," *IEEE Trans. Microw. Theory Techn.*, vol. 66, no. 7, pp. 3419–3432, Jul. 2018.

[9] X. Liu, W. Chen, L. Chen, F. M. Ghannouchi, and Z. Feng, "Linearization for hybrid beamforming array utilizing embedded over-the-air diversity feedbacks," *IEEE Trans. Microw. Theory Techn.*, vol. 67, no. 12, pp. 5235–5248, Dec. 2019.

[10] C. Li, S. He, F. You, J. Peng, and P. Hao, "Analog predistorter averaged digital predistortion for power amplifiers in hybrid beam-forming multi-input multi-output transmitter," *IEEE Access*, vol. 8, pp. 146145–146153, Aug. 2020.

[11] J. Sun, W. Shi, Z. Yang, J. Yang, and G. Gui, "Behavioral modeling and linearization of wideband RF power amplifiers using BiLSTM networks for 5G wireless systems," *IEEE Trans. Veh. Technol.*, vol. 68, no. 11, pp. 10348–10356, Nov. 2019.

[12] S. Hesami, S. R. Aghdam, C. Fager, T. Eriksson, R. Farrell, and J. Dooley, "Single digital predistortion technique for phased array linearization," in *Proc. IEEE Int. Symp. Circuits Syst. (ISCAS)*, May 2019, pp. 1–5.

[13] Z. Lu, S. Hairan, and G. Shujin, "A linearization method for phased array antenna based on DPD technology," in *Proc. 10th Int. Conf. Commun. Softw. Netw. (ICCSN)*, Jul. 2018, pp. 456–459.

[14] Q. Luo, C. Yu, and X.-W. Zhu, "A modified digital predistortion method for phased array transmitters with multi-channel time delay," in *IEEE MTT-S Int. Microw. Symp. Dig.*, Aug. 2018, pp. 1–3.

[15] S. Lee, M. Kim, Y. Sirl, E.-R. Jeong, S. Hong, S. Kim, and Y. H. Lee, "Digital predistortion for power amplifiers in hybrid MIMO systems with antenna subarrays," in *Proc. IEEE 81st Veh. Technol. Conf. (VTC Spring)*, May 2015, pp. 1–5.

[16] E. Ng, Y. Beltagy, P. Mitran, and S. Boumaiza, "Single-input single-output digital predistortion of power amplifier arrays in millimeter wave RF beamforming transmitters," in *IEEE MTT-S Int. Microw. Symp. Dig.*, Jun. 2018, pp. 481–484.

[17] X. Wang, C. Yu, Y. Li, W. Hong, and A. Zhu, "Real-time single channel over-the-air data acquisition for digital predistortion of 5G massive MIMO wireless transmitters," in *IEEE MTT-S Int. Microw. Symp. Dig.*, Aug. 2019, pp. 1–3.

[18] F. Jalili, F. F. Tafuri, O. K. Jensen, Y. Li, M. Shen, and G. F. Pedersen, "Linearization trade-offs in a 5G mmWave active phased array OTA setup," *IEEE Access*, vol. 8, pp. 110669–110677, 2020.

[19] L. Ding, G. T. Zhou, D. R. Morgan, Z. Ma, J. S. Kenney, J. Kim, and C. R. Giardina, "A robust digital baseband predistorter constructed using memory polynomials," *IEEE Trans. Commun.*, vol. 52, no. 1, pp. 159–165, Jan. 2004.

[20] J. Sun, J. Wang, L. Guo, J. Yang, and G. Gui, "Adaptive deep learning aided digital predistorter considering dynamic envelope," *IEEE Trans. Veh. Technol.*, vol. 69, no. 4, pp. 4487–4491, Apr. 2020.

[21] M. U. Hadi, P. A. Traverso, G. Tartarini, O. Venard, G. Baudoin, and J.-L. Polleux, "Digital predistortion for linearity improvement of VCSEL-SSMF-based radio-over-fiber links," *IEEE Microw. Wireless Compon. Lett.*, vol. 29, no. 2, pp. 155–157, Feb. 2019.

[22] W. Pan, C. Li, X. Quan, W. Ma, Y. Liu, S. Shao, and Y. Tang, "Digital linearization of multiple power amplifiers in phased arrays for 5G wireless communications," in *Proc. IEEE Int. Symp. Signal Process. Inf. Technol. (ISSPIT)*, Dec. 2018, pp. 247–251.

[23] *3rd Generation Partnership Project; Technical Specification Group Radio Access Network; Evolved Universal Terrestrial Radio Access (E-UTRA); Base Station (BS) Radio Transmission and Reception (Release 16)*, document 3GPP TS 36.104-1 V16.5.0,, May 2020.
[24] *3rd Generation Partnership Project; Technical Specification Group Radio Access Network; NR; Base Station (BS) Radio Transmission and Reception (Release 16)*, document 3GPP TS 38.104 V16.3.0, May 2020.
[25] N. Tervo, J. Aikio, T. Tuovinen, T. Rahkonen, and A. Parssinen, "Digital predistortion of amplitude varying phased array utilising over-the-air combining," in *IEEE MTT-S Int. Microw. Symp. Dig.*, Jun. 2017, pp. 1165–1168.
[26] B. Khan, N. Tervo, A. Parssinen, and M. Juntti, "Average linearization of phased array transmitters under random amplitude and phase variations," in *Proc. 16th Int. Symp. Wireless Commun. Syst. (ISWCS)*, Aug. 2019, pp. 553–557.
[27] E. Ng, Y. Beltagy, G. Scarlato, A. Ben Ayed, P. Mitran, and S. Boumaiza, "Digital predistortion of millimeter-wave RF beamforming arrays using low number of steering angle-dependent coefficient sets," *IEEE Trans. Microw. Theory Techn.*, vol. 67, no. 11, pp. 4479–4492, Nov. 2019.

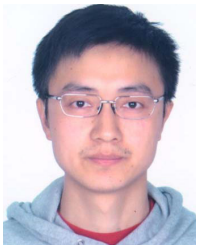

YING LIU (Member, IEEE) received the B.E. and M.S. degrees in communication engineering and the Ph.D. degree in communication and information systems from the University of Electronic Science and Technology of China (UESTC), in 2008, 2011, and 2016, respectively.

He has also worked as a Visiting Scholar with the Department of Electrical and Computer Engineering, Ohio State University (OSU), Columbus, OH, USA. He is currently an Assistant Professor with the National Key Laboratory of Science and Technology on Communications, UESTC. His research interests include wireless communication system design, nonlinear modeling, digital predistortion, full duplex communications, and signal processing in wireless communications.

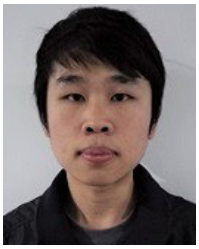

XIANGJIE XIA (Graduate Student Member, IEEE) was born in Anhui, China, in 1995. He received the B.E. degree in communication engineering from the University of Electronic Science and Technology of China (UESTC), Chengdu, China, in 2017, where he is currently pursuing the Ph.D. degree.

He is currently with the Key Laboratory of Science and Technology on Communications, UESTC. His research interests include interference suppression, linearization of high power amplifiers, and digital signal processing in wireless communications.

QIANNAN ZHANG was born in Henan, China, in 1995. She received the B.E. degree in communication engineering from the Henan University of China (UESTC), Kaifeng, China, in 2018, where she is currently pursuing the M.A. Eng. degree.

She is currently with the Key Laboratory of Science and Technology on Communications, UESTC. Her research interests include linearization of power amplifiers in multichannel transmitters and digital signal processing in wireless communications.

WENSHENG PAN (Member, IEEE) was born in Chongqing, China, in 1975. He received the B.E., M.S., and Ph.D. degrees in communication engineering from the University of Electronic Science and Technology of China (UESTC), in 1998, 2005, and 2015, respectively.

From 2005 to 2009, he has served as the Manager of NTS Technology, Inc. He is currently an Assistant Researcher with the National Key Laboratory of Science and Technology on Communications, UESTC. His research interests include power amplifier design, power amplifier linearization, digital predistortion, and crest factor reduction.

SHIHAI SHAO (Member, IEEE) was born in Liaoning, China, in 1980. He received the B.E. and Ph.D. degrees in communication and information systems from the University of Electronic Science and Technology of China, Chengdu, China, in 2003 and 2008, respectively. Since 2008, he has been with the National Key Laboratory of Science and Technology on Communications, UESTC, as a Professor. His research interests include full-duplex communications, signal processing in wireless communications, spread spectrum, and MIMO detection.

YOUXI TANG was born in Henan, China, in 1964. He received the B.E. degree in radar engineering from the College of PLA Ordnance, Shijiazhuang, China, in 1985, and the M.S. and Ph.D. degrees in communications and information systems from UESTC, Chengdu, China, in 1993 and 1997, respectively.

From 1998 to 2000, he was with the Huawei Technologies Company Ltd., Shanghai, China, as a Program Manager, working in the area of IS-95 mobile communications and third-generation mobile communications. Since 2000, he has been with the National Key Laboratory of Science and Technology on Communications, UESTC, as a Professor. His general research interests include spread spectrum systems and wireless mobile systems, with the emphasis on signal processing in communications.